Solute–Solvent Interactions in Aqueous Glycylglycine–CuCl$_2$ Solutions: Acoustical and Molecular Dynamics Perspective

Mysore Sridhar Santosh · Alexander Lyubartsev · Alexander Mirzoev · Denthaje Krishna Bhat

Abstract Acoustical and molecular dynamics studies were carried out to understand the various interactions present in glycylglycine–CuCl$_2$ aqueous solutions. Amongst these interactions, hydrogen bonding and solute–solvent interactions have been highlighted in this study. The radial distribution function (RDF) was used to investigate solution structure and hydration parameters. Binding of Cu^{2+} with various polar peptide atoms reveals the nature and degree of binding. The formation of complex clusters between glycylglycine and water molecules increases the relaxation time. The first hydration shell considerably influences the structure of the second shell, facilitating the formation of an ordered hydrogen bonded network. Both experimental and theoretical results have proved to be efficient in analyzing the behavior of molecules and to give a clear idea on molecular interactions in solutions.

Keywords Speed of sound · Molecular dynamics · CuCl$_2$ · Aqueous solutions

1 Introduction

In continuation of our earlier work [1–5] on the study of interactions between dipeptide and electrolytes in aqueous and aqueous ethanol systems, we present in this paper a new strategy to study solute–solvent interactions in glycylglycine–CuCl$_2$ aqueous solutions by experimental acoustics measurements and molecular dynamics simulations. Amino acids are the fundamental structural units of proteins. Among various biomolecules, amino acids are important food additives and have many applications in the pharmaceutical industries. They are also the building units of other complex biomolecules such as antibiotics and proteins. Metal ions play an important role in biological systems and the presence of copper–amino

M.S. Santosh · D.K. Bhat (✉)
Physical Chemistry Division, Department of Chemistry, National Institute of Technology Karnataka, Surathkal, Mangalore 575025, India
e-mail: denthajekb@gmail.com

A. Lyubartsev · A. Mirzoev
Division of Physical Chemistry, Department of Materials and Environmental Chemistry, Arrhenius Laboratory, Stockholm University, 10691, Stockholm, Sweden

acid complexes in human serum enhances the uptake of copper by liver tissue [6, 7]. Previous studies focused largely on the interactions between dipeptides and alkali or alkaline earth metals [8–12], but both theoretical and experimental work involving dipeptide and transition metal salts in aqueous solutions are very scant. Molecular dynamics simulation (MD) has proved to be a suitable complement to experiments for a quantitative description of physical and chemical phenomena involving metal ion solvation [13].

Acoustical properties of these model compounds (amino acids) together with electrolytes in aqueous solution provide information about solute–solvent and solute–solute interactions that can be of great help in understanding the effects of electrolytes on biomolecules [14–19]. Furthermore, H-bonding is of crucial importance in studies involving amino acids in aqueous solutions. The interactions of metal ions with the zwitterionic head groups of amino acids causes the transfer of hydrated water molecules to the bulk state. Also, water is known to be a indispensable matrix for the structural components and activities of living organisms. Thus, compounds containing hydroxyl and carbonyl groups are extensively hydrated in aqueous environments [20]. An interconnection between these groups can exist through hydrogen bonds [21, 22]. Indeed, the solvent water strongly influences the molecular structure of a compound [23]. A recent extension in the area of thermodynamics, by combining acoustical and simulation studies on the dynamics of electrolytes [24], has led us to study molecular interactions in the above systems. In the present work, an attempt is made to understand the interaction of glycylglycine–$CuCl_2$ in aqueous solutions by evaluating various acoustical parameters based on speed of sound measurements, and a comprehensive set of molecular dynamics simulations aimed at investigating molecular interactions between water, glycylglycine (GG), and $CuCl_2$, by analyzing the connection between molecular interactions and structural properties of this solute–solvent system.

2 Experimental

2.1 Materials

Glycylglycine and copper(II) chloride dihydrate of 99% purity for our studies were purchased from Sigma-Aldrich, Germany, Ltd. Commercially available glycylglycine of the highest purity was used without further purification. Copper(II) chloride dihydrate was used after drying for 72 h in a vacuum desiccator at room temperature. Deionized and doubly distilled degassed water with a specific conductance less than 1.29×10^{-6} $\Omega^{-1} \cdot cm^{-1}$ was used for the preparation of all solutions. The solutions were prepared on a mass basis by using a Mettler balance having a precision of ± 0.01 mg. Care was taken to avoid solvent evaporation and contamination during mixing. The temperature of the water bath was controlled within ± 0.01 K using a thermostat. In our studies, the concentration of $CuCl_2$ was kept constant at 0.25 mol·kg^{-1} while the molality of glycylglycine was varied. To prevent formation of air bubbles, all solutions were preheated in sealed Eppendorf tubes to 5°C above the measurement temperature, before filling the interferometer and densimetric cells.

2.2 Methods

Speeds of sound of the pure components and their mixtures were measured using a variable path, fixed frequency, interferometer provided by Mittal Enterprises, New Delhi (Model-83). It consists of a high frequency generator and a measuring cell. The frequency of the interferometer was fixed at 2 MHz. The capacity of the measurement cell was 7 mL. Cal-

Fig. 1 Structure of glycylglycine
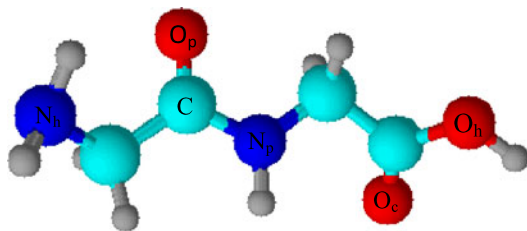
ibration of this ultrasonic interferometer was done by measuring the velocity in AR grade benzene and carbon tetrachloride. The maximum estimated error in the speed of sound measurements was found to be $\pm 0.08\%$. The temperature was controlled by circulating water around the liquid cell from a thermostatically-controlled and adequately stirred water bath. Densities were measured using a (Mettler Toledo) Density 30PX digital densitometer, with an uncertainty of $\pm 3 \times 10^{-3}$ kg·m^{-3}. The densitometer was calibrated using double distilled water and laboratory air. Viscosities were measured using a Brookfield DV-III Ultra Programmable Rheometer (Brookfield Engineering Laboratories, Inc., USA), which was calibrated using double-distilled water, and their uncertainty was found to be $\pm 0.5\%$. The sample and reference resonator cells with minimum volumes of 0.5 cm^3 were thermostatted with an accuracy of ± 0.01 K, and a previously described differential technique was employed for all measurements [25]. The physico-chemical parameters for glycylglycine–CuCl$_2$ aqueous solutions were measured at the temperatures 288.15 K, 298.15 K, 308.15 K, and 318.15 K. Each measurement was repeated thrice and the reported values are averages of all three trials.

2.3 Computational Methods

The structure of glycylglycine was computed using the all-atom AMBER force field (Version 4.1 from 1995), specially refined for protein simulations (Fig. 1) [26]. Partial atom charges were derived by electrostatic potential fitting from Hartree-Fock (6-31G*) computations of the optimized GG geometry, performed using the Gaussian-03 package [27]. Flexible SPC water by Toukan and Rahman [28] was used as a water model. For the Cu^{2+} ion, we used Lennard-Jones parameters, derived from the data on hydration free energies and diffraction structures in reference [29]. The Cl$^-$ anion was described by the Heinzinger parameter set [30].

The MD simulations were carried out using the general-purpose simulation package MDynaMix [31]. The double-time step method of Tuckerman et al. [32] was applied with 0.2 fs time step to describe fast motional modes, such as bond stretching, angular and torsional bending. Even short-range non-bonded interactions within 5 Å distance were treated with this faster time scale. The long-distance non-bonded interactions were integrated after each 2.0 fs. An Ewald summation was used to treat the long-range Columbic interactions. The cutoff distance in real space, R_{cut}, was optimized for maximum computational performance and was equal to $R_{cut} = 11.0$ Å, and the Ewald parameter α was taken as $2.8/R_{cut}$. Simulations were carried out in the NPT ensemble using periodic boundaries. The coupling of temperature and pressure was established by means of a Nose-Hoover thermo-barostat, with relaxation times of 30 and 700 fs for the temperature and pressure fluctuations, respectively. During the first 0.2 ns of simulation, glycylglycine molecule was kept fixed, allowing the equilibration of water molecules and ions in the system. The system was further equilibrated during the next 0.3 ns of simulation where all of the atoms in glycylglycine were

Fig. 2 Variation of the speed of sound, u, with concentration for glycylglycine–CuCl$_2$ aqueous solutions at different temperatures: 288.15 K, ■; 298.15 K, ●; 308.15 K, ▲; 318.15 K, ▼

Fig. 3 Variation of density, ρ, with concentration for glycylglycine–CuCl$_2$ aqueous solutions at different temperatures: 288.15 K, ■; 298.15 K, ●; 308.15 K, ▲; 318.15 K, ▼

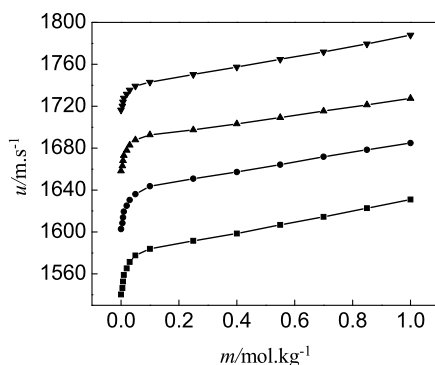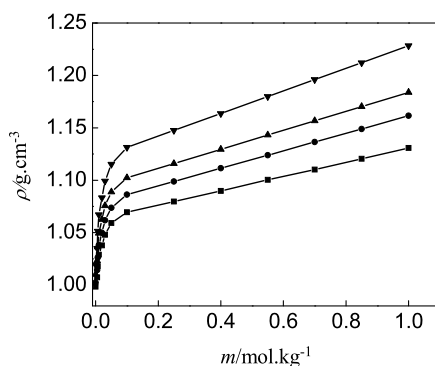allowed to move. Then, production runs were carried out for a further 9.5 ns, leading to a total simulation length of 10 ns. The temperature was kept constant at 298.15 K and pressure at 1 atm during all simulations. The simulated system contained 500 water molecules, 2 glycylglycine molecules, 5 Cu^{2+} ions and 10 Cl$^-$ ions. The radial distribution function (RDF) is traditionally used to analyze solution structure revealed by either experimental or computer simulation studies. The RDF function $g(ij, r)$ describes the relative probability of finding a pair of atoms i and j at a distance r apart, compared to a completely random distribution at the same solution density [33]. The appropriately normalized running integral of the RDF gives the number of atoms j (and hence the number of molecules that they belong to) in a sphere of radius r around the atom i, which can be used to define the coordination number (traditionally by using the position of the first RDF minimum).

3 Results and Discussion

The experimental values of the speed of sound, density and viscosity for glycylglycine–CuCl$_2$ aqueous solutions at $T = (288.15$ to $318.15)$ K are given in Table 1 and shown in Figs. 2, 3 and 4. The calculated parameters namely, isentropic compressibility, acoustic impedance, hydration number, intermolecular free length, classical sound absorption, and shear relaxation time for the solutions are given in Table 2.

The isentropic compressibilities were calculated using the following equation:

$$\kappa_S = 1/(u^2\rho) \tag{1}$$

Table 1 Speed of sound (u), density (ρ) and viscosity (η) values for glycylglycine–CuCl$_2$ aqueous solutions at different temperatures and concentrations

m/mol·kg^{-1}	u/m·s^{-1}	ρ/g·cm^{-3}	η/mPa·s
	T/K = 288.15		
0.000	1540.28	0.9984	1.49
0.005	1546.51	1.0072	1.53
0.007	1552.74	1.0180	1.58
0.010	1558.97	1.0290	1.62
0.020	1565.20	1.0378	1.67
0.030	1571.43	1.0480	1.73
0.050	1577.63	1.0592	1.79
0.100	1583.92	1.0694	1.86
0.250	1591.64	1.0796	1.94
0.400	1598.57	1.0898	2.02
0.550	1606.83	1.1004	2.10
0.700	1614.39	1.1102	2.19
0.850	1622.74	1.1204	2.27
1.000	1630.90	1.1307	2.35
	T/K = 298.15		
0.000	1602.84	1.0023	1.27
0.005	1608.38	1.0142	1.31
0.007	1613.92	1.0261	1.35
0.010	1619.46	1.0380	1.39
0.020	1625.09	1.0499	1.43
0.030	1630.54	1.0618	1.47
0.050	1636.08	1.0737	1.54
0.100	1643.66	1.0862	1.60
0.250	1650.83	1.0988	1.69
0.400	1657.12	1.1114	1.77
0.550	1664.23	1.1239	1.85
0.700	1671.73	1.1365	1.93
0.850	1678.36	1.1489	2.01
1.000	1684.92	1.1615	2.09
	T/K = 308.15		
0.000	1658.16	1.0101	1.11
0.005	1663.12	1.0232	1.15
0.007	1668.06	1.0363	1.19
0.010	1673.02	1.0494	1.23
0.020	1677.94	1.0625	1.27
0.030	1682.88	1.0756	1.31
0.050	1687.82	1.0887	1.35
0.100	1692.78	1.1023	1.42
0.250	1697.37	1.1159	1.52
0.400	1703.14	1.1295	1.60
0.550	1709.26	1.1431	1.68
0.700	1715.38	1.1567	1.76
0.850	1721.27	1.1703	1.85
1.000	1727.45	1.1839	1.93

Table 1 (*Continued*)

$m/\text{mol·kg}^{-1}$	$u/\text{m·s}^{-1}$	$\rho/\text{g·cm}^{-3}$	$\eta/\text{mPa·s}$
	$T/\text{K} = 318.15$		
0.000	1716.41	1.0192	0.90
0.005	1720.23	1.0350	0.94
0.007	1724.03	1.0514	0.98
0.010	1727.84	1.0671	1.02
0.020	1731.67	1.0833	1.06
0.030	1735.40	1.0992	1.10
0.050	1739.26	1.1153	1.15
0.100	1743.02	1.1314	1.22
0.250	1750.38	1.1475	1.29
0.400	1757.46	1.1637	1.37
0.550	1764.78	1.1799	1.44
0.700	1771.83	1.1960	1.52
0.850	1779.56	1.2121	1.59
1.000	1787.92	1.2283	1.68

Fig. 4 Variation of viscosity, η, with concentration for glycylglycine–CuCl$_2$ aqueous solutions at different temperatures: 288.15 K, ■; 298.15 K, ●; 308.15 K, ▲; 318.15 K, ▼
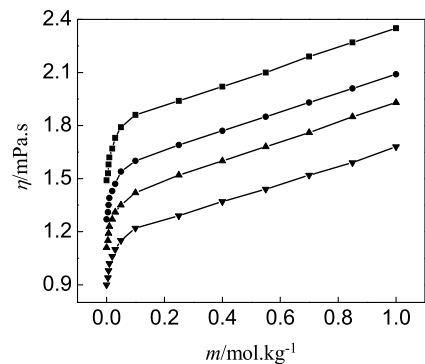
while the hydration number was computed using the relation:

$$n_{\text{h}} = \left(\frac{n_1}{n_2}\right)\left(1 - \frac{\kappa_S}{\kappa_S^0}\right) \tag{2}$$

where κ_S and κ_S^0 are the adiabatic compressibilities of solution and pure solvent, respectively, and n_1 and n_2 are number of moles of solvent and solute, respectively.

Classical sound absorption and shear relaxation time were calculated using the equations:

$$\frac{\alpha}{f^2} = \frac{8\pi^2\eta}{3\rho u^2} \tag{3}$$

$$\tau = \frac{4\eta}{3\rho u^2} \tag{4}$$

where ρ and η are the density and viscosity of the solution, and f is the frequency of the ultrasonic wave.

Table 2 Isentropic compressibility (κ_S), specific acoustic impedance (Z), hydration number (n_h), intermolecular free length (L_f), classical sound absorption (α/f^2) and shear relaxation time (τ) values for glycylglycine–CuCl$_2$ aqueous solutions at different temperatures and concentrations

m/ mol·kg^{-1}	$\kappa_S \times 10^{-10}$/ N^{-1}·m^2	$Z \times 10^5$/ kg·m^{-2}·s^{-1}	n_h	L_f/ Å	$\alpha/f^2 \times 10^{-15}$/ s^2·m^{-1}	$\tau \times 10^{13}$/ s
			$T/K = 288.15$			
0.000	4.22	1537.8	0.0	0.3969	1.6538	8.3872
0.005	4.15	1557.6	6.1	0.3935	1.6698	8.4685
0.007	4.07	1580.6	5.8	0.3901	1.6924	8.5832
0.010	3.99	1604.1	5.9	0.3867	1.7030	8.6370
0.020	3.93	1624.3	6.0	0.3832	1.7269	8.7579
0.030	3.86	1646.8	6.3	0.3798	1.7575	8.9132
0.050	3.79	1671.0	5.7	0.3764	1.7851	9.0532
0.100	3.72	1693.8	5.8	0.3730	1.8227	9.2436
0.250	3.65	1718.3	6.0	0.3695	1.8649	9.4577
0.400	3.59	1742.1	6.1	0.3660	1.9070	9.6711
0.550	3.51	1768.1	5.8	0.3626	1.9433	9.8552
0.700	3.45	1792.2	5.8	0.3592	1.9899	10.0917
0.850	3.38	1818.1	5.9	0.3557	2.0222	10.2587
1.000	3.32	1844.0	6.1	0.3523	2.0543	10.4185
			$T/K = 298.15$			
0.000	3.88	1606.5	0.0	0.3894	1.29666	6.5760
0.005	3.81	1631.2	5.7	0.3860	1.31272	6.6574
0.007	3.74	1656.0	5.9	0.3825	1.32795	6.7347
0.010	3.67	1680.9	6.1	0.3791	1.34239	6.8079
0.020	3.60	1706.1	6.0	0.3756	1.35592	6.8765
0.030	3.54	1731.3	6.2	0.3722	1.36903	6.9430
0.050	3.47	1756.6	5.8	0.3687	1.40874	7.1444
0.100	3.40	1785.3	5.7	0.3653	1.43347	7.2698
0.250	3.33	1813.9	6.1	0.3618	1.48376	7.5249
0.400	3.27	1841.7	5.9	0.3584	1.52474	7.7327
0.550	3.21	1870.4	6.0	0.3550	1.56250	7.9242
0.700	3.14	1899.9	5.8	0.3516	1.59756	8.1020
0.850	3.08	1928.2	5.7	0.3481	1.63285	8.2809
1.000	3.03	1957.0	6.0	0.3445	1.66636	8.4509
			$T/K = 308.15$			
0.000	3.60	1674.9	0.0	0.3816	1.05077	5.3289
0.005	3.53	1701.7	6.2	0.3780	1.06830	5.4178
0.007	3.47	1728.6	5.9	0.3744	1.08502	5.5027
0.010	3.40	1755.6	5.7	0.3708	1.10094	5.5834
0.020	3.34	1782.8	6.0	0.3671	1.11615	5.6605
0.030	3.28	1810.1	5.8	0.3635	1.13062	5.7339
0.050	3.21	1837.5	6.2	0.3599	1.14439	5.8037
0.100	3.15	1865.9	6.0	0.3563	1.18192	5.9941
0.250	3.08	1894.0	6.1	0.3527	1.24299	6.3038
0.400	3.02	1923.6	5.8	0.3490	1.28391	6.5113
0.550	2.95	1953.8	5.9	0.3454	1.32254	6.7073
0.700	2.89	1984.1	5.8	0.3418	1.35948	6.8946
0.850	2.83	2014.4	6.1	0.3382	1.40274	7.1140
1.000	2.76	2045.1	6.0	0.3345	1.43626	7.2840

Table 2 (*Continued*)

$m/$ mol·kg^{-1}	$\kappa_S \times 10^{-10}/$ N^{-1}·m^2	$Z \times 10^5/$ kg·m^{-2}·s^{-1}	n_h	$L_f/$ Å	$\alpha/f^2 \times 10^{-15}/$ s^2·m^{-1}	$\tau \times 10^{13}/$ s
			$T/K = 318.15$			
0.000	3.33	1749.3	0.0	0.3733	0.78803	3.9965
0.005	3.26	1780.4	5.9	0.3697	0.80689	4.0921
0.007	3.19	1812.6	6.1	0.3661	0.82446	4.1812
0.010	3.13	1843.7	6.2	0.3625	0.84176	4.2690
0.020	3.07	1875.9	6.0	0.3589	0.85788	4.3507
0.030	3.02	1907.5	5.7	0.3553	0.87361	4.4305
0.050	2.96	1939.7	5.9	0.3517	0.89614	4.5448
0.100	2.90	1972.0	6.1	0.3481	0.93312	4.7323
0.250	2.84	2008.5	6.2	0.3445	0.96465	4.8922
0.400	2.78	2045.1	5.9	0.3409	1.00210	5.0821
0.550	2.72	2082.2	5.8	0.3373	1.03024	5.2248
0.700	2.66	2119.1	6.0	0.3337	1.06431	5.3976
0.850	2.60	2157.0	5.9	0.3301	1.08902	5.5229
1.000	2.54	2196.1	6.0	0.3265	1.12489	5.7048

3.1 Speed of Sound

It is observed from Fig. 2 that the speed of sound increases with an increase in the glycyl-glycine concentration, suggesting greater association among the molecules in the studied solutions [34]. This may be due to intermolecular hydrogen bonding between the solute and solvent molecules and dipole–dipole interactions. Hydrogen bonds among water molecules break with increasing temperature and consequently more monomeric water molecules are formed. The vacant space present in the cage-like water structure is occupied by broken water molecules that thus get trapped. Upon addition of glycylglycine to aqueous CuCl$_2$ solutions, the interactions between water and CuCl$_2$ decreases. This results in a lower compressibility between the molecules present in the solution. As a result, the polar molecules of glycylglycine form more compact structures with the water molecules through intermolecular hydrogen bonding [35]. Consequently, a decrease in compressibility is favored. The solution is predominantly composed of water–water interactions which form the typical three-dimensional cage-like structure of water, and the increased association observed in the above solutions may also be due to water structure enhancement brought about by an increase in electrostriction in the presence of CuCl$_2$. Likewise, formation of a compact structure of zwitterions–water dipoles and zwitterions–ion in solution also leads to an increase in the ultrasonic velocity and a decrease in compressibility. However, with a corresponding increase in compressibility, the mean distance between the molecules tends to increase. Thus, the net decrease in compressibility is a result of these two opposing tendencies.

3.2 Isentropic Compressibility

When an ion enters a solvent's environment, solvent molecules from the bulk solvent are attracted towards the ion due to the electrostrictive force. Because to this, there is a decrease in the number of available solvent molecules for the next incoming ion and, hence, this process is called compression. Every solvent has a limit for its compression called the limiting

compressibility value. However, the volumetric concentration of the solution increases with a decrease in compressibility of the solvent, since the solution compressibility is lower than that of the solvent. Furthermore, the electrostrictive forces cause a breakage in the water structure with increasing solute concentration and compact packing occurs with the water molecules surrounding the solute, reducing the compressibility. In aqueous glycylglycine–CuCl$_2$ solutions, it is observed (Table 2) that the isentropic compressibilities decrease with an increase in the glycylglycine concentration and temperature. Hence, there exist strong solute–solvent interactions through dipole–dipole and acceptor-donor interactions of the –OH group of glycylglycine with the surrounding water molecules [35, 36]. In addition, chelation of Cu^{2+} to the terminal amino group and peptide nitrogen takes place, leading to simultaneous coordination with the carboxyl oxygens.

3.3 Specific Acoustic Impedance

The acoustic impedance of a medium can be defined as the ratio of the instantaneous pressure excess on any particle of the medium to the instantaneous velocity of that particle [37]. The specific acoustic impedance is dependent on both concentration and temperature of the solution. Variations of pressure from one particle to another occur when an acoustic wave travels in a medium. The inertial and elastic properties of the medium govern this factor. As the internal pressure and cohesive energy [38] increases with solute concentration, strong intermolecular hydrogen bonding occurs between glycylglycine and water molecules. Hence, an increase in specific acoustic impedance is caused by an increase in instantaneous pressure excess at any molecule (glycylglycine–CuCl$_2$ in aqueous solution) with propagation of a sound wave (Table 2). It is to be noted that the copper–glycylglycine complex is formed by bonding between Cu(II) and the amino group of glycylglycine. Thermodynamic studies have reported the simultaneous coordination of a peptide oxygen [39, 40] with replacement of two water molecules by the chelating ring around the Cu(II) ion. In the Cu(II)–glycylglycine complex, the ligand is coordinated by three donor atoms: the amino nitrogen, the deprotonated peptide nitrogen and the carboxylate oxygen atoms. The short bond length in Cu(II)–glycylglycine complexes can be attributed to the strong bonding between Cu(II) and the deprotonated peptide nitrogen. In order to stabilize the above bond, simultaneous coordination of the carboxylate group takes place [41, 42]. Further, to counterbalance the stabilization effect of carboxylate coordination on copper(II)–peptide N bonding, a competition arises between the hydroxide ion with strong donor properties and the deprotonated peptide nitrogen atom.

3.4 Effect of Hydration

The Frank and Wen model [43] explains the hydration of solute molecules in water on the basis of solute–solvent interactions; it pictures three different solvent structural regions in the neighborhood of the solute. As a result of electrostrictive and other attractive forces exerted by the solute, a layer of immobilized and compressed water is formed just outside the molecule. Consequently, a slightly less compressed or structure-broken region of water molecules, distantly affected by these forces, surrounds this layer. The outermost layer of bulk water possesses the typical tetra-coordinated hydrogen-bonded structure of water that is not affected by any other forces. Changes in the first two layers of the solvent around the solute molecule are indicated by compressibility measurements. The water structure is slightly disturbed by the hydrogen-bonded network around the solute in the case of glycylglycine; this bonding holds the water around the solute firmly, making the hydration layer even less

Fig. 5 RDFs between chloride ion and water hydrogens and water oxygens for glycylglycine–CuCl$_2$ aqueous solution
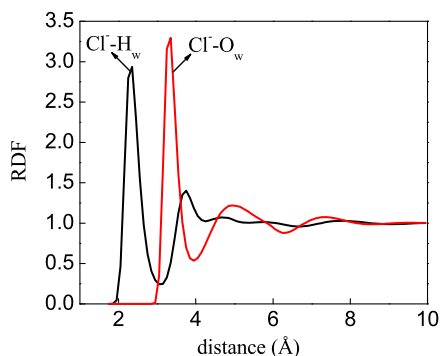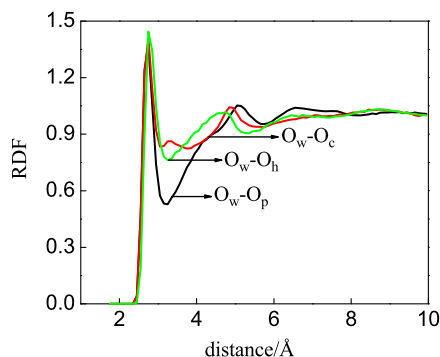

Fig. 6 RDFs between water oxygen and polar atoms of the GG dipeptide: O$_p$ of the peptide carbonyl; O$_c$ of COOH (carbonyl); O$_h$ of hydroxyl oxygen

compressible [23]. From the n_h values of glycylglycine reported in Table 2, it is found that each glycylglycine molecule is closely bound and forms a complex in a cluster. The Cu^{2+} ion, having the hydration number 6, indicates that Cu^{2+} has less affinity for Cl$^-$ as compared to water molecules. In contrast, Cl$^-$ ions are electrostatically attracted by water hydrogens, which is consistent with the distance of closest approach between the water hydrogens and Cl$^-$. From the RDFs for H$_w$–Cl and O$_w$–Cl (Fig. 5), it is observed that the positions of the first peaks of O$_w$–Cl and H$_w$–Cl differ by about 1 Å, and the first peak of H$_w$–Cl suggests that the hydrogens form almost linear bridges between the chloride and oxygens.

The RDFs of water oxygen and peptide oxygens (O$_p$, O$_c$, O$_h$) are shown in Fig. 6. At a distance of 2.9 Å, the O$_w$–O$_p$ distribution function approaches a maximum with a co-ordination number around 2. This distribution function is an indication of hydrogen bonds between an acceptor atom of the solute and donors of water molecules with the oxygen of the peptide C=O group strongly hydrogen bonded with two water molecules. The structural organization and dynamics of water molecules, coupled to the molecular interfaces, are highly dependent on inter-molecular hydrogen bonding. Also, the functionality of peptides is determined by the formation and breaking of such hydrogen bonds. The RDF between O$_w$–O$_c$ has a peak very similar to the corresponding peak of O$_p$, showing two water molecules bound by hydrogen bonds to the carbonyl oxygen. The O$_w$–O$_c$ RDF has, however, a second maximum at about 4 Å distance, which is absent in the O$_w$–O$_p$ RDF. This maximum evidently comes from waters bound to the hydroxyl oxygen of glycylglycine. Nevertheless, the glycylglycine–water RDFs depend very little on the concentration of ions or of glycylglycine. The probable reason for this is that the strong electric field of divalent ions pulls some of the water molecules away from glycylglycine, resulting in small shifts of the RDFs.

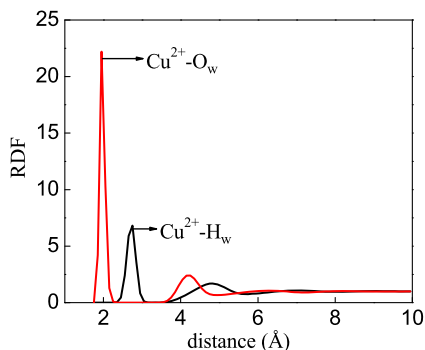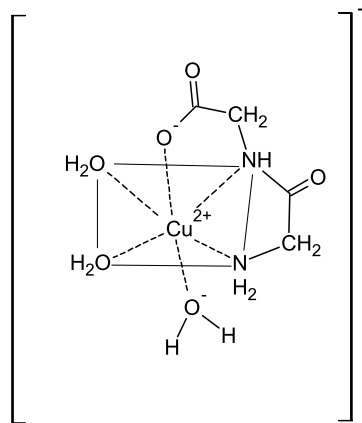**Fig. 7** RDFs between Cu^{2+} ions and water oxygens and water hydrogens

Fig. 8 Predicted structure of the Cu^{2+}–glycylglycine complex


The O_w–O_h RDF has a higher intensity, which is explained by a contribution from an oxygen atom of another water molecule bound to the hydroxyl hydrogen, as well as due to other water molecules occasionally appearing near the peptide COOH group.

The RDFs of Cu^{2+}–O_w and Cu^{2+}–H_w are shown in Fig. 7. The first peak of the Cu^{2+}–O_w RDF is centered at 2.08 Å. The second peak of this function, related to second hydration shell, appears at a 4.2 Å, clearly separated from the first coordination sphere. That the Cu^{2+}–H_w RDF peaks occur at larger distances with respect to the corresponding oxygen peaks indicates that, especially in the first shell, the water molecules are fairly well dipole-oriented with the dominant ion–water interactions occurring with their oxygen atoms pointing to the ionic center. Apparently, the second solvation sphere is considerably influenced by the first hydration shell, leading to a more ideally ordered hydrogen-bond network between water molecules across the first two hydration shells. The structure of the predicted Cu–glycylglycine complex [40] is shown in Fig. 8. This figure helps in understanding the nature of binding between Cu^{2+} and glycylglycine molecules as discussed above.

3.5 Intermolecular Free Length

The intermolecular free length shows a behavior similar to the compressibility values. As observed in Table 2, the decrease in intermolecular free length results in closer packing of molecules. The decrease in intermolecular free length causes an increase in ultrasonic

Fig. 9 RDFs between Cu^{2+} ions and polar atoms of the GG dipeptide: O_p of the peptide carbonyl; O_c of COOH (carbonyl); O_h of the hydroxyl oxygen
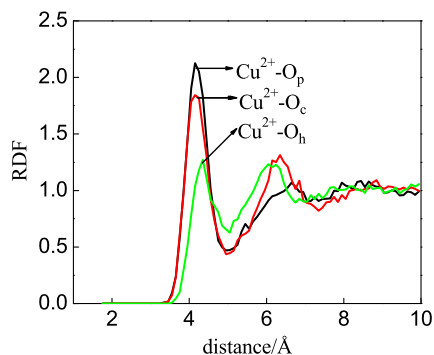
velocity. This behavior indicates the presence of dipole–dipole and acceptor–donor interactions between the solute and solvent molecules, suggesting a structure-promoting tendency of glycylglycine–$CuCl_2$ in aqueous solutions [23]. Further, water molecules bound to Cu^{2+} have hydrogen atoms directed away from the ion. One of these hydrogens can form a hydrogen bond to the carbonyl oxygen of glycylglycine, building the configuration C=O–water–Cu^{2+}. With water in the first coordination shell of Cu^{2+}, one can speculate that it might be easier to form a hydrogen bond to the carbonyl oxygen of glycylglycine than with other water molecules. The RDFs between the polar atoms of peptide (O_p, O_C and O_h) and Cu^{2+} ion are shown in Fig. 9. One can see that the overall RDF structure for all three peptide oxygen atoms with Cu^{2+} is rather similar but they differ in their intensities. As seen from Fig. 9, Cu^{2+}–O_p has the maximum intensity, which indicates stronger binding with the oxygen atom. In contrast, Cu^{2+}–O_h has the lowest intensity, which indicates weaker binding with the hydroxyl oxygen in the carboxyl group. Copper bound to the oxygen of the carboxyl group, i.e., the Cu^{2+}–O_c RDF, shows a second maximum at about 6 Å, which in fact corresponds to ions bound to the peptide carbonyl oxygen O_p. One can conclude from the above RDFs that Cu^{2+} binds to the peptide oxygen (O_p) stronger than the carbonyl or hydroxyl oxygens present in the carboxyl group. Hence, the degree of binding is a result of a very delicate balance between many competing interactions such as ion–water, water–water, water–dipeptide, and dipeptide–ion.

3.6 Sound Absorption and Relaxation Time

The variation of classical sound absorption with respect to the glycylglycine concentration is reported in Table 2. The presence of intermolecular association through hydrogen bonding between the solute and solvent molecules is strongly supported by the gradual increase in sound absorption. This may be explained as follows: when glycylglycine and $CuCl_2$ are added to water, the molecules of glycylglycine may break the structure of associated water molecules in aqueous $CuCl_2$ and form (glycylglycine–$CuCl_2$–water) complex clusters between the unlike molecules through intermolecular hydrogen bonds. Due to dipole-dipole [44] and Debye forces (dipole-induced-dipole), the water–water hydrogen bonding is strengthened. Consequently, stronger viscous forces (decrease in freedom of molecular rotation) are present between solute–solvent and solvent–solvent molecules in the aqueous solutions. When the concentration of glycylglycine is gradually increased in water, the number of hydrogen bonding sites available for bonding also increases, resulting in large numbers of O–H···O bonds between added glycylglycine and water molecules. Hence, in order to break the large number of intermolecular hydrogen bonds, more sound energy is utilized.

The linear increase in relaxation time with glycylglycine concentration (Table 2) is due to reinforcement of hydrogen bonds in water-forming complex clusters between glycylglycine and a fixed number of water molecules. The hydrogen bonds are weakened at higher temperature due to thermal vibrations and structure breaking effects that predominate over the formation of hydrogen bonds. As a result, the τ value decreases for the glycylglycine–$CuCl_2$ complex in aqueous solution. One can note that Cu^{2+} binds to glycylglycine strongly, as a consequence of the degree of binding being a very delicate balance between many competing interactions (Cu^{2+}–water, water–water, water–glycylglycine, and glycylglycine–Cu^{2+}).

4 Conclusions

A systematic acoustical study of glycylglycine–$CuCl_2$ aqueous solutions has been carried out at different concentrations and temperatures. The RDFs obtained from MD simulations are concordant with the experimental studies and also support the discussion. The acoustical data give valuable information on solute-solvent interactions in solutions. There is a uniform decrease in the classical sound absorption and shear relaxation time with increase in temperature, indicating the weakening of intermolecular forces due to thermal agitation of the molecules at higher temperatures. The above results clearly explain the variations due to dipole–dipole interactions, hydrogen bonding, and the C=O–water–cation configuration. These conclusions give scope for further studies on the structure, intermolecular interactions, density and temperature effects on solute–solvent interactions for glycylglycine in aqueous electrolyte solutions through modeling and simulations.

References

1. Santosh, M.S., Bhat, D.K., Bhatt, A.S.: Molecular interactions in glycylglycine–$MnCl_2$ aqueous solutions at (288.15, 293.15, 298.15, 303.15, 308.15, 313.15, and 318.15) K. J. Chem. Eng. Data **54**, 2813–2818 (2009)
2. Santosh, M.S., Bhatt, A.S., Bhat, D.K.: Physico-chemical, acoustic and excess properties of glycylglycine–$MnCl_2$ in aqueous ethanol mixtures at different temperatures. Fluid Phase Equilib. **291**, 174–179 (2010)
3. Santosh, M.S., Bhat, D.K., Bhatt, A.S.: Molecular Interactions between glycylglycine and $Mn(COOCH_3)_2$ in aqueous and aqueous ethanol mixtures. J. Chem. Eng. Data **56**, 768–782 (2011)
4. Santosh, M.S., Bhat, D.K., Bhatt, A.S.: Ultrasonic velocities, densities, and viscosities of glycylglycine and $CoCl_2$ in aqueous and aqueous ethanol systems at different temperatures. J. Chem. Thermodyn. **42**, 742–751 (2010)
5. Santosh, M.S., Bhat, D.K., Bhatt, A.S.: Volumetric, refractometric, and excess properties of glycylglycine in aqueous $FeCl_2$ solution at temperatures T = (288.15 to 318.15) K. J. Chem. Eng. Data **55**, 4048–4053 (2010)
6. Kober, P.A., Haw, A.B.: Spectrophotometric study of copper complexes and the biuret reaction. J. Am. Chem. Soc. **38**, 457–472 (1916)
7. El-Eazby, M.S., Al-Hasan, J.M., Eweiss, N.F., Al-Massaad, F.: Cobalt(II), nickel(II), and copper(II) complexes of di-and tetrapeptides containing tyrosine and glycine residues. Can. J. Chem. **57**, 104–112 (1979)
8. Perkyns, J.S., Wang, Y., Pettitt, B.M.: Salting in peptides: conformationally dependent solubilities and phase behavior of a tripeptide zwitterion in electrolyte solution. J. Am. Chem. Soc. **118**, 1164–1172 (1996)

9. Kohtani, M., Jarrold, M.F., Wee, S., O'Hair, R.A.: Metal ion interactions with polyalanine peptides. J. Phys. Chem. B **108**, 6093–6097 (2004)

10. Imai, T., Kinoshita, M., Hirata, F.: Salt effect on stability and solvation structure of peptide: an integral equation study. Bull. Chem. Soc. Jpn. **73**, 1113–1122 (2000)

11. Thomas, A.S., Elcock, A.H.: Molecular dynamics simulations of hydrophobic associations in aqueous salt solutions indicate a connection between water hydrogen bonding and the Hofmeister effect. J. Am. Chem. Soc. **129**, 14887–14898 (2007)

12. Wong, C.H.S., Ma, N.L., Tsang, C.W.: A theoretical study of potassium cation binding to glycylglycine (GG) and alanylalanine (AA) dipeptides. Chem. Eur. J. **8**, 4909–4918 (2002)

13. Rode, B.M., Schwenk, C.F., Tongraar, A.: Structure and dynamics of hydrated ions—new insights through quantum mechanical simulations. J. Mol. Liq. **110**, 105–122 (2004)

14. Hippel, P.H.V., Schleich, T.: In: Timasheff, S.N., Fasman, G.D. (eds.) Structure and Stability of Biological Macromolecules, vol. 2, p. 417. Marcel Dekker, New York (1969)

15. Romero, C.M., Moreno, E., Rojas, J.L.: Apparent molal volumes and viscosities of DL-α-alanine in water–alcohol mixtures. Thermochim. Acta **328**, 33–38 (1999)

16. Kumar, A.: Alternate view on thermal stability of the DNA duplex. Biochemistry **34**, 12921–12925 (1995)

17. Tamura, Y., Gekko, K.: Compactness of thermally and chemically denatured ribonuclease A as revealed by volume and compressibility. Biochemistry **34**, 1878–1884 (1995)

18. Rai, T.C., Yan, G.B.: Viscosity B-coefficients and activation parameters for viscous flow of a solution of heptanedioic acid in aqueous sucrose solution. Carbohydr. Res. **338**, 2921–2927 (2003)

19. Badaryani, R., Kumar, A.: Ionic interactions from volumetric investigations of L-alanine in NaBr, KCl, KBr and MgCl$_2$ up to high concentrations. Fluid Phase Equilib. **201**, 321–333 (2002)

20. Chalikian, T.V.: Structural thermodynamics of hydration. J. Phys. Chem. B **105**, 12566–12578 (2001)

21. Scheiner, S.: Hydrogen Bonding: A Theoretical Perspective, pp. 52–290. Oxford University Press, Oxford (1997)

22. Jeffrey, G.A.: An Introduction to Hydrogen Bonding. Oxford University Press, Oxford (1997)

23. Raman, Ponnuswamy V., Kolandaivel, P., Perumal, K.: Ultrasonic and computational study of intermolecular association through hydrogen bonding in aqueous solutions of D-mannitol. J. Mol. Liq. **135**, 46–52 (2007)

24. Ribeiro, M.C.C.: Polarization effects in molecular dynamics simulations of glass-formers Ca(NO$_3$)$_2 \cdot n$H$_2$O, $n = 4$, 6, and 8. J. Chem. Phys. **132**, 134512–134521 (2010)

25. Riyazuddeen, Bansal G.K.: Intermolecular/interionic interactions in L-leucine–, L-asparagine–, and glycylglycine–aqueous electrolyte systems. Thermochim. Acta **445**, 40–48 (2006)

26. Cornell, W.D., Cieplak, P., Bayly, C.I., Gould, I.R., Merz, K.M., Ferguson, D.M., Spellmeyer, D.C., Fox, T., Caldwell, J.W., Kollman, P.: A second generation force field for the simulation of proteins, nucleic acids, and organic molecules. J. Am. Chem. Soc. **117**, 5179–5197 (1995)

27. Frisch, M.J., Trucks, G.W., Schlegel, H.B., Scuseria, G.E., Robb, M.A., Cheeseman, J.R., Montgomery, J.A. Jr., Vreven, T., Kudin, K.N., Burant, J.C., Millam, J.M., Iyengar, S.S., Tomasi, J., Barone, V., Mennucci, B., Cossi, M., Scalmani, G., Rega, N., Petersson, G.A., Nakatsuji, H., Hada, M., Ehara, M., Toyota, K., Fukuda, R., Hasegawa, J., Ishida, M., Nakajima, T., Honda, Y., Kitao, O., Nakai, H., Klene, M., Li, X., Knox, J.E., Hratchian, H.P., Cross, J.B., Bakken, V., Adamo, C., Jaramillo, J., Gomperts, R., Stratmann, R.E., Yazyev, O., Austin, A.J., Cammi, R., Pomelli, C., Ochterski, J.W., Ayala, P.Y., Morokuma, K., Voth, G.A., Salvador, P., Dannenberg, J.J., Zakrzewski, V.G., Dapprich, S., Daniels, A.D., Strain, M.C., Farkas, O., Malick, D.K., Rabuck, A.D., Raghavachari, K., Foresman, J.B., Ortiz, J.V., Cui, Q., Baboul, A.G., Clifford, S., Cioslowski, J., Stefanov, B.B., Liu, G., Liashenko, A., Piskorz, P., Komaromi, I., Martin, R.L., Fox, D.J., Keith, T., Al-Laham, M.A., Peng, C.Y., Nanayakkara, A., Challacombe, M., Gill, P.M.W., Johnson, B., Chen, W., Wong, M.W., Gonzalez, C., Pople, J.A.: Gaussian 03, Revision E.01. Gaussian, Inc., Wallingford (2004)

28. Toukan, K., Rahman, A.: Molecular-dynamics study of atomic motions in water. Phys. Rev. B **31**, 2643–2648 (1985)

29. Babu, C.S., Lim, C.: Empirical force fields for biologically active divalent metal cations in water. J. Phys. Chem. A **110**, 691–699 (2006)

30. Heizinger, K.: Computer simulations of aqueous electrolyte solutions. Physica **131B**, 196–216 (1985)

31. Lyubartsev, A.P., Laaksonen, A.: MDynaMix—a scalable portable parallel MD simulation package for arbitrary molecular mixtures. Comput. Phys. Commun. **128**, 565–589 (2000)

32. Allen, M.P., Tidesley, D.J.: Computer Simulation of Liquids. Clarendon Press, Oxford (1987)

33. Laaksonen, A., Kusalik, P.G., Svishchev, I.M.: Three-dimensional structure in water–methanol mixtures. J. Phys. Chem. A **101**, 5910–5918 (1997)

34. Kharat, S.J.: Density, viscosity and ultrasonic velocity studies of aqueous solutions of sodium acetate at different temperatures. J. Mol. Liq. **140**, 10–14 (2008)

35. Rao, N.P., Verrall, R.E.: Ultrasonic velocity, excess adiabatic compressibility, apparent molar volume, and apparent molar compressibility properties of binary liquid mixtures containing 2-butoxyethanol. Can. J. Chem. **65**, 810–816 (1987)
36. Nikam, P.S., Ansari, H.R., Hasan, M.: Acoustical properties of fructose and maltose solutions in water and in aqueous 0.5 M NH_4Cl. J. Mol. Liq. **84**, 169–178 (2000)
37. Awasthi, A., Rastogi, M., Gupta, M., Shukla, J.P.: Ultrasonic investigation of molecular association in ternary mixtures. J. Mol. Liq. **80**, 77–88 (1999)
38. Palani, R., Jayachitra, K.: Ultrasonic study of ternary electrolytic mixtures at 303, 308 and 313 K. Indian J. Pure Appl. Phys. **46**, 251–254 (2008)
39. Planka, T.S., Rockenbauer, A., Korecz, L.: ESR study of the copper(II)–glycylglycine equilibrium system in fluid aqueous solution. Computer analysis of overlapping multispecies spectra. Magn. Reson. Chem. **37**, 484–492 (1999)
40. Kim, M.K., Martell, A.E.: Copper(II) complexes of glycylglycine. Biochemistry **3**, 1169–1174 (1964)
41. Farkas, E., Kiss, T.: Effects of side-chain donor groups on deprotonation of peptide amide in copper(II) complexes at high pH. Polyhedron **8**, 2463–2467 (1989)
42. Brookes, G., Pettit, L.D.: Thermodynamics of complex formation between hydrogen, copper(II), and nickel (II) ions and dipeptides containing non-coordinating substituent groups. J. Chem. Soc. Dalton Trans. 2106–2112 (1975)
43. Smirnov, P.R., Trostin, V.N.: Structural parameters of Cu^{2+} aqua complexes in aqueous solutions of its salts. Russ. J. Gen. Chem. **79**, 1591–1599 (2009)
44. Raman, M.S., Ponnuswamy, V., Kolandaivel, P., Perumal, K.: Ultrasonic and DFT study of intermolecular association through hydrogen bonding in aqueous solutions of D(–)-arabinose. J. Mol. Liq. **151**, 97–106 (2010)